

Selective area grown ZnTe nanowires as the basis for quasi-one-dimensional CdTe-HgTe multishell heterostructures

J. Hajer^{1,*}, W. Mantei¹, M. Kessel¹, C. Brüne^{1,†}, S. Wenner^{2,3}, A. T. J. van Helvoort², H. Buhmann¹, and L. W. Molenkamp¹

¹*Institute for Topological Insulators and Physikalisches Institut (EP3), Universität Würzburg, Am Hubland, 97074 Würzburg, Germany*

²*Department of Physics, Norwegian University of Science and Technology (NTNU), 7491 Trondheim, Norway*

³*Materials and Nanotechnology, SINTEF Industry, 7465 Trondheim, Norway*



(Received 27 August 2018; revised manuscript received 21 April 2020; accepted 8 May 2020; published 1 June 2020)

Selective area growth is employed in the vapor-liquid-solid molecular beam epitaxy of ZnTe nanowire arrays. Full control over the location of the individual nanowires is achieved by defined positioning of the growth catalyst. This study addresses the influence of substrate material and growth temperature on the yield of vertical nanowires. The optimized procedure provides arrays of single-crystalline free-standing nanowires with a high ensemble uniformity. The nanowires exhibit a uniform shape with a diameter of about 80 nm and reach a length of more than 3 μm , which makes them suitable as substrates for core-shell nanowires of the topological insulator material HgTe.

DOI: [10.1103/PhysRevMaterials.4.066001](https://doi.org/10.1103/PhysRevMaterials.4.066001)

I. INTRODUCTION

The fabrication of nanowire heterostructures often requires precise control of the geometric properties such as the morphology and areal density. For III-V semiconductors, the position-controlled growth of homogeneous nanowire arrays is well established [1,2], but reports on similar growth techniques for II-VI nanowires are rare. II-VI nanowires are investigated mainly for their extraordinary optical and magnetic properties [3,4], more recently extended to quasi-one-dimensional topological insulators based on HgTe nanowire shells [5].

Typically, nanowire growth is seeded by liquid metallic droplets via the vapor-liquid-solid (VLS) [6] mechanism [4,7]. Heating a thin layer of Au on top of a GaAs substrate, e.g., creates self-organized Au-Ga droplets with poor uniformity. Nanowires then grow with a nonuniform diameter, and their rather dense distribution obscures the subsequent overgrowth. Prepositioning the VLS growth seeds provides a much higher degree of control in terms of diameter and areal density. It is commonly realized by a preceding lithographical patterning step. This approach has been demonstrated successfully for III-V nanowires [8] but has limitations with II-VI materials. The rather low growth temperature of II-VI nanowires requires alloying of the metallic growth seed with, typically, a group-III element such as Ga to form a liquid droplet [5,7].

In this paper, we discuss the selective area growth of ZnTe nanowires and their application as a substrate for the radial

overgrowth with CdTe and HgTe. We investigate the influence of surface preparation, the substrate material, and the substrate temperature. The growth parameters are further optimized with respect to the nanowire length and the areal uniformity. We analyze the structural quality of the nanowires and finally demonstrate radial overgrowth with a shell consisting of CdTe and HgTe.

II. METHODS

In the following, we give a general description of the selective area growth process for ZnTe nanowires. The starting point of the process is a lithographically patterned array of Au disks. The Au disks are fabricated by electron beam lithography and have a height of 25 nm and a diameter of 70 nm. Since a clean surface is crucial, an Ar ion milling step is applied immediately prior to the Au evaporation. Oxygen plasma cleaning followed by an HCl dip assures the removal of carbon contamination related to the lithography. The samples are then transferred into an ultrahigh vacuum cluster connecting amongst others three molecular beam epitaxy (MBE) chambers optimized for the growth of III-V compounds, wide gap II-VI materials, and Hg containing layers, respectively.

In the III-V chamber, Ga is supplied for 2 min at a beam equivalent pressure of about 4×10^{-8} mbar from an effusion cell at a substrate temperature of 250 °C. Solid-state diffusion of Ga into the Au disks results in the formation of Au-Ga alloy droplets with a melting temperature of about 350 °C. Upon transferral into the II-VI chamber, the substrates are heated in a stabilizing Zn flux to the growth temperature of 440–450 °C, well above the melting point of the Au-Ga alloy. The temperature is monitored by band edge thermometry [9,10], which allows us to adjust the temperature of the substrate surface with high precision and reliability. ZnTe nanowires are grown using beam-equivalent pressures in the

*jhajer@physik.uni-wuerzburg.de

†Present address: Center for Quantum Spintronics, Department of Physics, Norwegian University of Science and Technology (NTNU), 7491 Trondheim, Norway.

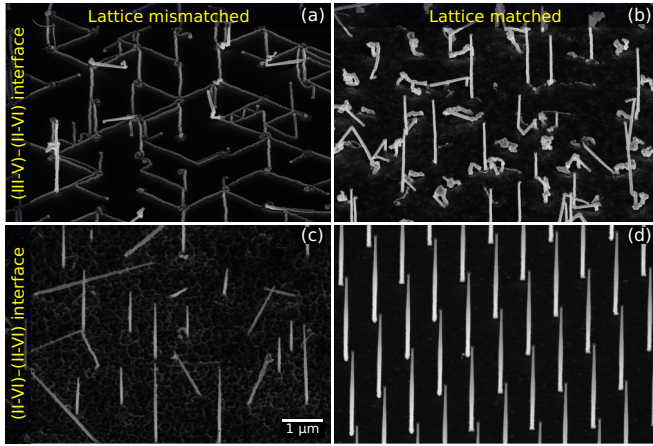


FIG. 1. ZnTe nanowires are grown under similar conditions at 440 °C on diverse (111)B substrate materials: (a) GaAs, (b) InAs, (c) ZnSe, and (d) ZnTe. These materials cover the different possible options regarding lattice mismatch and type of interface to the nanowire.

range of $1\text{--}2 \times 10^{-6}$ mbar and a Zn : Te ratio of 0.6–0.7 at a constant substrate temperature. For the final radial overgrowth with CdTe and HgTe, the samples are transferred into the Hg-containing MBE chamber.

III. NANOWIRE GROWTH INVESTIGATION

The first question we address is how the choice of the substrate material influences the ZnTe nanowire growth. Thus, we examine different configurations, including lattice matched and mismatched growth, as well as (III-V)–(II-VI) and (II-VI)–(II-VI) interfaces. Arrays of Au–Ga growth seeds are prepared on GaAs, InAs, ZnSe, and ZnTe (111)B substrates, where InAs, ZnSe, and ZnTe substrates are provided as 1- μ m-thick MBE-grown layers on GaAs. Figure 1 summarizes the results. On GaAs, Fig. 1(a), the percentage of vertical wires is almost zero. We attribute this observation to the fact that the large lattice mismatch of 7.6% between GaAs and ZnTe [11] does not favor vertical wire growth, which additionally is strongly influenced by the unsaturated bonds at the (III-V)–(II-VI) interface. For InAs as well as for ZnSe substrates, we observe only little improvement compared with GaAs. While the InAs substrate is nearly lattice matched but still exhibits dangling bonds at the interface, the ZnSe substrate provides a crystallographically correct interface but again does not match the lattice constant. Both parameters appear to be essential for the growth of straight and free-standing nanowires. For the homoepitaxial growth of ZnTe nanowires on a ZnTe substrate, both parameters are matched and we observe an almost perfect yield of vertical nanowire growth [cf. Fig. 1(d)]. A thorough removal of lithography-related carbon contamination prior to nanowire growth has proved to be crucial for high quality nanowire growth. A two-step cleaning process with oxygen plasma and HCl assures a reproducible high sample quality.

Important for radial overgrowth of the ZnTe nanowires is the length and shape. For both, the important parameter is the substrate temperature and its constancy during growth. In our growth study, the substrate temperature has been varied in

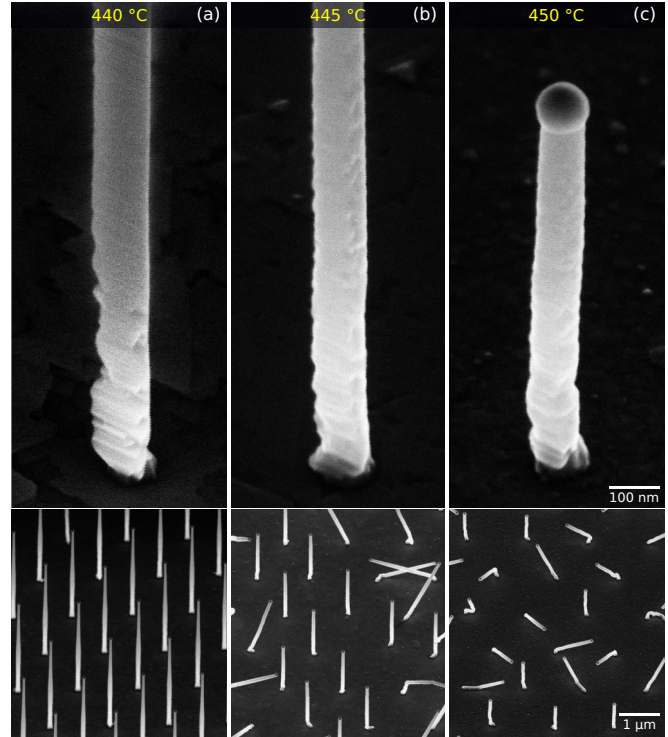


FIG. 2. ZnTe nanowires are grown under similar conditions at different substrate temperatures: (a) 440 °C, (b) 445 °C, and (c) 450 °C. The top images show an electron micrograph of a single nanowire, images at the bottom give an overview at lower magnification.

the range between 400 and 455 °C. For temperatures below 440 °C, the nanowires tend to kink and grow in various higher-indexed directions. Above 450 °C, the growth rate significantly slows down and the yield of vertical wires is low. The temperature window between 440–450 °C is thus favorable for the nanowire growth. Figure 2 summarizes the results for 440, 445, and 450 °C. Depending on the temperature, differences in morphology can be observed. For 440 °C, Fig. 2(a), we obtain a very uniform array of nanowires pointing along the vertical [111]B direction. The cross section at the lower part of the nanowire appears to be triangular. For a slightly higher substrate temperature [445 °C, Fig. 2(b)], the yield of vertical nanowires reduces and the cross section develops additional facets and appears more circular. For 450 °C, Fig. 2(c), the yield decreases further but the shape becomes more and more circular. At this temperature, the growth rate is already very slow, which makes it hard to achieve nanowires exceeding 1 μ m length. These results show that by adjusting the substrate temperature, we are able to control the cross-sectional shape of the nanowires. However, a more circular cross section, which is favorable for the subsequent overgrowth, reduces the yield and the length of well oriented wires.

Generally, we observe a change in the surface roughness of the nanowires along their entire length. While the tip region appears rather smooth, the bottom part becomes rough. To investigate the crystal quality over the length of the nanowires, a bunch of nanowires grown at a substrate

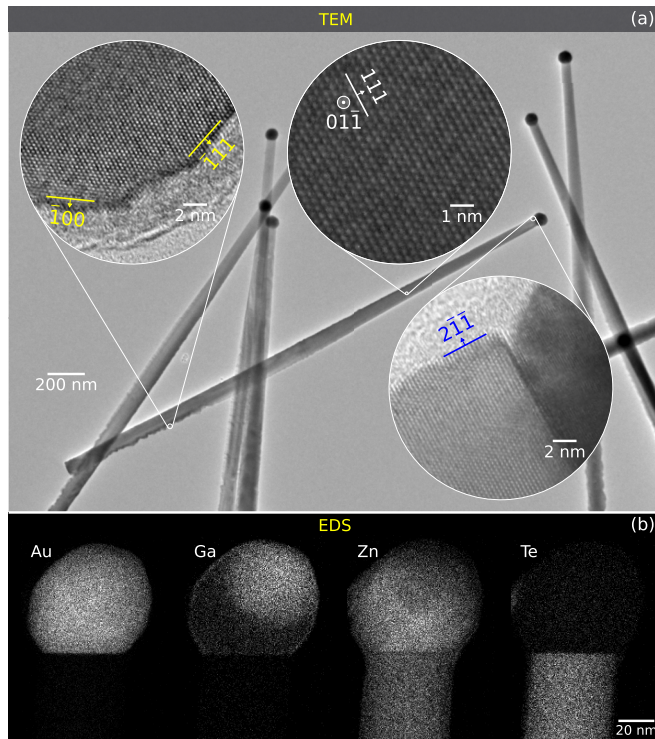


FIG. 3. A transmission electron micrograph of a ZnTe nanowire is shown in (a), the insets are higher resolution images recorded at different positions along the wire. (b) shows elemental maps of the nanowire's tip obtained by energy dispersive spectroscopy.

temperature of 440 °C has been prepared for transmission electron microscopy (TEM) investigation, shown in Fig. 3(a). The diffraction contrast is homogeneous along the entire length and comparable for different nanowires. This already indicates that the wires consist of a single crystal phase. High resolution imaging reveals a zinc-blende crystal structure with almost no lattice defects over the entire length [cf. insets in Fig. 3(a)], and no signs of polytypism (the formation of wurtzite segments in the zinc-blende lattice often observed in VLS-grown nanowires [12]). Comparing the terminating side facets of tip and base, we find that the lower part mostly consists of low-indexed $\langle 111 \rangle$ and $\langle 100 \rangle$ facets (marked in yellow), while the upper part exhibits $\langle 211 \rangle$ facets (blue) parallel to the growth direction. We relate this observation to the following fact: The base of the nanowires is exposed to the rather high substrate temperature for several hours. Therefore, it is most likely that the observed roughness in the vicinity of the nanowire base arises from the formation of low-indexed facets due to thermal dissociation and redistribution of material throughout growth.

The TEM measurements also allow us to additionally investigate the element distribution within the nanowires by energy dispersive spectroscopy. Figure 3(b) shows the distribution of Au, Ga, Zn, and Te in the vicinity of the nanowire tip. The nanowire itself consists exclusively of Zn and Te. Au and Ga are not detected within the nanowire and can only be found in the metallic droplet at the tip. This is a clear indication that both materials act solely as a catalyst for the nanowires and are not incorporated in the nanowire. Furthermore, while Au

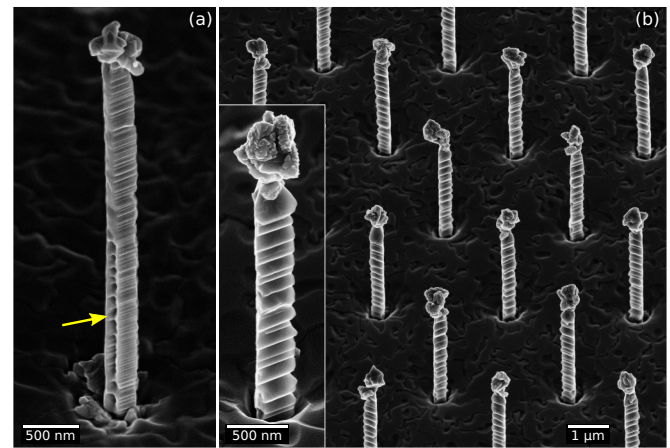


FIG. 4. The images show CdTe-HgTe shells on ZnTe core nanowires with (a) trigonal and (b) more circular cross section at the nanowire base. The arrow in (a) points out a gap in the HgTe shell.

seems to be homogeneously distributed within the droplet, Ga appears to occur in two different concentrations. This points to a noneutectic Au-Ga alloy which solidifies in two phases with different stoichiometry during cool down [13]. Additionally, a significant amount of Zn is found in the droplet, which at the same time is nearly free of Te. This is consistent with the anticipated VLS growth mechanism for self-organized ZnTe nanowires [4], where Zn is dissolved within the droplet while Te is transported to the growth front mostly by surface processes.

In a final step, the ZnTe nanowire array is used for the growth of a tubular quasi-one-dimensional topological insulator based on HgTe. This requires overgrowth of the ZnTe nanowires with a CdTe buffer layer. CdTe provides a lattice constant which induces the required strain in the subsequent epitaxially grown HgTe [14] to open a bulk band gap [15,16]. Due to the large lattice mismatch of 6.1% between ZnTe and CdTe [11], the CdTe shell is assumed to be fully relaxed after few nanometers. CdTe overgrowth shows good results within a substrate temperature window of 320–330 °C for a balanced Cd : Te ratio with beam equivalent pressures of $1-2 \times 10^{-6}$ mbar. The HgTe shell is grown at a substrate temperature of 190 °C with a Hg beam equivalent pressure of $2-5 \times 10^{-4}$ mbar and a Hg : Te ratio of 220–250. Figure 4 shows scanning electron micrographs of core-shell nanowires for (a) a triangular- and (b) a more circular-shaped ZnTe core. Both samples exhibit pronounced steplike side facets that have already been analyzed and reported for self-organized CdTe-HgTe core-shell nanowires [5,14] and are attributed to stable facets of the HgTe crystal. Another typical feature for HgTe nanowires with a triangular-shaped core is that the HgTe shell appears to not be homogeneously closed [cf. arrow in Fig. 4(a)]. Figure 5 shows electron micrographs of the cross section of a cleaved nanowire with a triangular core. Figure 5(a) is taken with an energy-selective detector for backscattered electrons (EsB) and provides information about both surface topography and material contrast. Simultaneously, Fig. 5(b) is recorded with an InLens detector, which primarily images the topography. Figure 5(a) clearly allows us to distinguish the bright HgTe shell from the darker

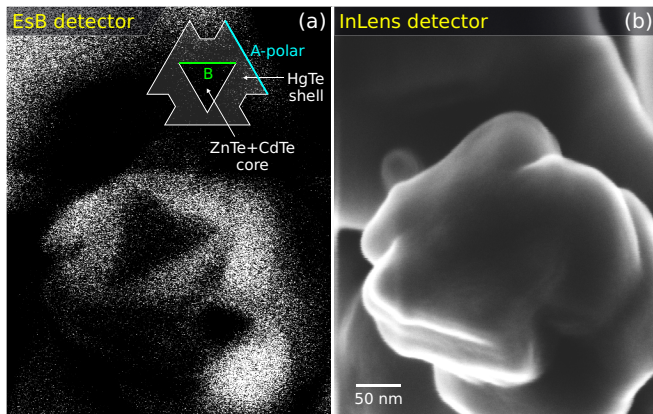


FIG. 5. Scanning electron micrographs of a cleaved ZnTe-CdTe/HgTe core-shell nanowire grown at 450 °C are shown, simultaneously recorded with (a) EsB and (b) InLens detector. A qualitative cross section of the nanowire is sketched as an inset, highlighting the polarity of the prominent side facets of core and shell.

ZnTe-CdTe core. The dominant side facets of core and shell are rotated by 60°. An illustrating sketch is given in the inset of Fig. 5(a). In a previous work, we have shown that the HgTe shell develops its stable facets on the A-polar sides [5], while the ZnTe core has B-polar side facets. This leads to preferred overgrowth at the edges of the core rather than

on its side facets, resulting in an irregular shape of the HgTe shell. Hence, a closed HgTe shell overgrowth is challenging on the B-polar side facets of a trigonal core nanowire. For circular cross sections, we achieve completely closed HgTe shells over the entire length of the nanowire, as shown in Fig. 4(b). However, already, a slight variation in the beam equivalent pressure ratio results in the formation of a gap on the B-polar sides of these nanowires also.

IV. SUMMARY AND CONCLUSION

We have developed a process for the selective area growth of ZnTe nanowire arrays by VLS-MBE. The optimization of growth with respect to length and morphology provides an optimal nanowire template for overgrowth with the topological insulator HgTe. We are able to grow a prepatterned array of more than 3- μm -long ZnTe nanowires. The high crystal quality is confirmed by TEM investigations. The shape of the nanowires is controllable by the growth temperature, which allows for the fabrication of closed-shell quasi-one-dimensional topological insulators based on HgTe.

ACKNOWLEDGMENTS

We gratefully acknowledge the financial support of the ERC Advanced Grant (project 4-TOPS), the DFG (SFB Project No. 1170, SPP Project No. 1666, Leibniz-Preis, ct.qmat), and the Bayerisches Staatsministerium für Bildung und Kultus, Wissenschaft und Kunst (ENB IDK TOIS, ITI).

- [1] K. Tomioka, Y. Kobayashi, J. Motohisa, S. Hara, and T. Fukui, *Nanotechnology* **20**, 145302 (2009).
- [2] H. J. Fan, P. Werner, and M. Zacharias, *Small* **2**, 700 (2006).
- [3] D. Ferrand, J. Cibert, A. Wasiela, C. Bourgonon, S. Tatarenko, G. Fishman, T. Andrearczyk, J. Jaroszyński, S. Koleśnik, T. Dietl, B. Barbara, and D. Dufeu, *Phys. Rev. B* **63**, 085201 (2001).
- [4] T. Wojtowicz, E. Janik, W. Zaleszczyk, J. Sadowski, G. Karczewski, P. Dłużewski, S. Kret, W. Szuszkiewicz, E. Dynowska, J. Domagala, M. Aleszkiewicz, L. T. Baczewski, A. Petrouchik, A. Presz, W. Pacuski, A. Golnik, P. Kossacki, J. F. Morhange, H. Kirmse, W. Neumann, and W. Caliebe, *J. Korean Phys. Soc.* **53**, 3055 (2008).
- [5] M. Kessel, J. Hajer, G. Karczewski, C. Schumacher, C. Brüne, H. Buhmann, and L. W. Molenkamp, *Phys. Rev. Mater.* **1**, 023401 (2017).
- [6] R. S. Wagner and W. C. Ellis, *Appl. Phys. Lett.* **4**, 89 (1964).
- [7] E. Janik, J. Sadowski, P. Dłużewski, S. Kret, L. T. Baczewski, A. Petrouchik, E. Lusakowska, J. Wrobel, W. Zaleszczyk, G. Karczewski, T. Wojtowicz, and A. Presz, *Appl. Phys. Lett.* **89**, 133114 (2006).
- [8] L. E. Jensen, M. T. Björk, S. Jeppesen, A. I. Persson, B. J. Ohlsson, and L. Samuelson, *Nano Lett.* **4**, 1961 (2004).
- [9] M. B. Denton, W. L. Johnson, and M. D. Sirkis, Method of wafer band-edge measurement using transmission spectroscopy and a process for controlling the temperature uniformity of a wafer, United States Patent No. US6891124B2, January 5, 2001.
- [10] R. Schlereth, J. Hajer, L. Fürst, S. Schreyeck, H. Buhmann, and L. W. Molenkamp, *J. Cryst. Growth* **537**, 125602 (2020).
- [11] *Semiconductors—Basic Data*, edited by O. Madelung (Springer, Berlin, 1996).
- [12] P. Caroff, J. Bolinsson, and J. Johansson, *IEEE J. Sel. Top. Quantum Electron.* **17**, 829 (2011).
- [13] R. P. Elliott and F. A. Shunk, *Bull. Alloy Phase Diagrams* **2**, 356 (1981).
- [14] M. Kessel, L. Lunczer, N. Tarakina, C. Schumacher, H. Buhmann, and L. W. Molenkamp, *Appl. Phys. Lett.* **114**, 153104 (2019).
- [15] C. Brüne, C. X. Liu, E. G. Novik, E. M. Hankiewicz, H. Buhmann, Y. L. Chen, X. L. Qi, Z. X. Shen, S. C. Zhang, and L. W. Molenkamp, *Phys. Rev. Lett.* **106**, 126803 (2011).
- [16] L. Fu, C. L. Kane, and E. J. Mele, *Phys. Rev. Lett.* **98**, 106803 (2007).